

Nonlinear Femtosecond Pulse Reshaping in Waveguide Arrays

Darren D. Hudson^{1*}, **Kimberlee Shish**², **Thomas R. Schibli**¹, **J. Nathan Kutz**²,
Demetrios N. Christodoulides³, **Roberto Morandotti**⁴, and **Steven T. Cundiff**¹

¹ *JILA, National Institute of Standards and Technology
and University of Colorado, Boulder, CO 80309-0440*

² *Department of Applied Mathematics,
University of Washington, Seattle, WA 98195-2420*

³ *College of Optics and Photonics, CREOL, University of Central Florida,
4000 Central Florida Boulevard, Orlando, FL 32816*

⁴ *Institut National de la Recherche Scientifique, Université du Québec,
1650 Boulevard Lionel Boulet, J3X 1S2, Varennes, Canada*

* *Department of Physics, University of Colorado, Boulder, CO 80309-0390*

(Dated: November 18, 2018)

We observe nonlinear pulse reshaping of femtosecond pulses in a waveguide array due to coupling between waveguides. Amplified pulses from a mode-locked fiber laser are coupled to an AlGaAs core waveguide array structure. The observed power-dependent pulse reshaping agrees with theory, including shortening of the pulse in the central waveguide.

© 2018 Optical Society of America

OCIS codes: 190.7110, 190.6135

Waveguide arrays have proven to be an ideal testbed for nonlinear optical waves in discrete systems. Much of the work done on these devices has focused on the spatial aspects of the output light field [1, 2, 3, 4]. The physics that determines the spatial profile of the transmitted beam is quite rich and suitable to theoretical treatment via the discrete nonlinear Schrödinger equation. This nonlinear equation can be tailored to include many physical processes that are present in the waveguide array such as discrete diffraction, normal dispersion, and self-phase modulation. Many novel spatial phenomena have been demonstrated using a waveguide array including discrete spatial solitons [1, 2], discrete modulational instability [3], and optical discrete surface solitons [4].

Despite the fact that most of these experiments used pulses to achieve the necessary peak powers, temporal effects have largely been neglected. Recently, the formation of X-waves was demonstrated in waveguide arrays [5, 6, 7]. The general structure observed was attributed to the interplay between discrete diffraction, normal dispersion, and the nonlinear Kerr effect. Here, we demonstrate nonlinear pulse shortening in a waveguide array. We carefully examine how the pulse shape in each waveguide depends on peak power of the input pulse using intensity autocorrelation. The output of the central waveguide shows significant shortening for high peak power due to attenuation of its lower power wings, as predicted recently [8]. The energy in the wings shifts to the outer waveguides. Thus, the waveguide array is acting as an effective saturable absorber. Understanding the temporal reshaping in the waveguide will be critical for future work involving these devices, such as using the waveguide array as a pulse resaper in optical telecommunication systems or as an intensity discriminator inside a mode-locked laser [9]. Simulations of the governing coupled-mode equations corroborate the observed experimental pulse-shaping results.

Coupled-mode theory provides an analytic reduction of the governing equations describing the propagation of electromagnetic energy in waveguides and waveguide arrays [10]. The theory assumes that the electromagnetic field is localized transversely in each waveguide and that the exchange of energy between the waveguides can be accurately modeled by an evanescent, linear coupling. When intense electromagnetic fields induce self-phase modulation, coupled-mode theory can be modified to include the nonlinear index of refraction [1]. The resulting nonlinear coupled-mode theory agrees well with experiment [2, 11, 12, 13]. To leading-order, the nearest-neighbor coupling of electromagnetic energy in the waveguide array is included in the discretely coupled nonlinear Schrödinger equations

$$i\frac{\partial A_n}{\partial z} - \frac{\beta''}{2} \frac{\partial^2 A_n}{\partial t^2} + \gamma |A_n|^2 A_n + c(A_{n+1} + A_{n-1}) = 0. \quad (1)$$

where A_n represents the normalized electric field amplitude in the n^{th} waveguide ($n = -N, \dots, -1, 0, 1, \dots, N$ and there are $2N + 1$ waveguides). We take the linear coupling coefficient to be $c = 0.82 \text{ mm}^{-1}$ and the nonlinear self-phase modulation parameter to be $\gamma = 3.6 \text{ m}^{-1}\text{W}^{-1}$. The parameter $\beta'' = 1.25 \text{ ps}^2/\text{m}$ is the experimentally measured chromatic dispersion in the waveguide array. The simulations of Eq. (1) that follow are performed with 41 ($N = 20$) waveguides [13] for various launch powers that match experimental conditions. A pseudo-spectral method is implemented that spectrally transforms the time-domain solution and uses a fourth-order Runge-Kutta for propagation in the waveguide.

To generate the input pulses, we use a mode-locked, Erbium doped fiber laser with a repetition rate of 25 MHz (operating at 1550nm) and a chirped-pulse amplifier/compressor system (see Fig. 1). Using dispersion compensating fiber (DCF), the normally chirped pulses from the fiber laser are further broadened to several picoseconds to avoid nonlinearities in the amplifier. These stretched pulses are coupled to a bi-directionally pumped Erbium amplifier [14], which increases the pulse energy by a factor of 7, while maintaining the original pulse shape. The output of the amplifier is temporally compressed/stretched in free-space by a diffraction grating compressor. The compressor is adjusted to produce 600 fs pulses (FWHM as measured by autocorrelation), which are normally chirped and 3.8 times the Fourier transform limit. The output pulse energy is 3.5 nJ.

The pulses are coupled into the waveguide array using standard microscope objectives (40x) mounted on 3-axis stages. The input field is mode matched to the waveguide with a coupling efficiency $> 60\%$, corresponding to a peak power of 1.5 kW. The waveguide array has a $10 \mu\text{m}$ center-to-center spacing between waveguides, with $1.5 \mu\text{m}$ tall ridges and $4 \mu\text{m}$ wide waveguides. Index guiding in the vertical direction is provided by a core layer consisting of $\text{Al}_{0.18}\text{Ga}_{0.82}\text{As}$ and cladding layers consisting of $\text{Al}_{0.24}\text{Ga}_{0.76}\text{As}$.

To verify that discrete spatial solitons are forming and to estimate the coupling coefficient between adjacent waveguides, the output power distribution of the array was measured as a function of input power (see Fig. 2). The energy localizes in the center waveguides for high power due to discrete self-focusing in the waveguide array [2]. At low power, the input light easily couples to neighboring waveguides and thus yields a nearly uniform power in each waveguide at the output end.

To measure the temporal reshaping effects of the waveguide array, background free auto-correlations are performed on the output of each waveguide. The autocorrelation measurements are performed in the crossed-beam geometry with a thin BBO crystal used for Type-1 second harmonic generation (SHG). A translation stage provides a scanning delay, while a 16-bit digitizer records the SHG signal detected by a photomultiplier tube. The data traces are continuously scanned and averaged. For reference, an autocorrelation of the input pulse is also recorded.

Fig. 3 shows the pulse reshaping effects of the waveguide array at each of the input powers, with experimental results on the left and numerical simulation of Eq. (1) on the right. At a peak power of 400 W, the output pulses from the central and outer waveguides were essentially identical to the input pulse (Fig 3-(a) and (d)). In this regime the γ term is negligible. The weak pulse launched into the center waveguide evanescently couples to neighboring waveguides. Thus, at the output multiple copies of the input pulse can be observed in each waveguide. As the input power is increased to 720 W ((b) and (e)), the pulse reshaping of the central waveguide begins to emerge. At the highest input power (1.5 kW) the γ term in Eq. (1) becomes non-negligible and the peak of the pulse decouples from neighboring waveguides. Meanwhile, the low intensity wings of the pulse are coupled to the nearest neighbor waveguides. The result is a shortened pulse in the center waveguide with the wings removed in agreement with the predicted nonlinear pulse shortening [8]. Fig. 3-(c),(f) shows the output of the waveguide array at high power. The triple peaked autocorrelation of the outer waveguides in Fig. 3-(c),(f) is evidence of a double peaked pulse shape. The experimental results agree well with the numerical simulation at each power level.

Taking a closer look at the central waveguide pulse shape as a function of input power (Fig. 4) shows the reshaping increases strongly at high peak power. In Fig. 4, a 600 fs pulse was launched into the central waveguide and the output autocorrelation of the central waveguide was measured as a function of input power. The output pulse for the highest power case shows a pulse width of less than half that of the input pulse. To determine how much of the pulse reshaping could be due to dispersive recompression of the pulse in the waveguide, the dispersion of the waveguide was measured to be around 1250 fs²/mm using white-light interferometry. Given the length of the waveguide array, dispersion should only change the pulse length by around 60 fs, well below the change observed (>300 fs). Also, a

purely chromatic dispersion compression [8] would be independent of the peak power in the waveguide.

In summary, we have observed nonlinear pulse shortening in a waveguide array and theoretically matched the experimental results by numerically solving Eq. (1). This phenomenon could have a wide range of applications involving pulse reshaping for long distance telecommunications and emerging photonic technologies. In addition, understanding this pulse reshaping will be crucial for any mode-locked laser system using waveguide array technology as an effective saturable absorber. Future work will include a detailed measurement of the pulse reshaping as a function of the coupling coefficient between waveguides.

J. N. Kutz acknowledges support from the National Science Foundation(DMS-0604700). The authors would also like to thank M.M. Feng and J.K. Wahlstrand for technical assistance, and A. D. Bristow for useful discussions.

References

1. D.N. Christodoulides and R.I. Joseph, “Discrete self-focusing in nonlinear arrays of coupled waveguides,” *Opt. Lett.* **13**, 794 (1988).
2. H.S. Eisenberg, Y. Silberberg, R. Morandotti, A.R. Boyd and J. S. Aitchison, “Discrete Spatial Optical Solitons in Waveguide Arrays,” *Phys. Rev. Lett.* **81**, 3383 (1998).
3. J. Meier, G. I. Stegeman, D. N. Christodoulides, Y. Silberberg, R. Morandotti, H. Yang, G. Salamo, M. Sorel, and J.S. Aitchison, “Experimental Observation of Discrete Modulational Instability,” *Phys. Rev. Lett.* **92**, 163902 (2004).
4. S. Suntsov, K.G. Makris, D.N. Christodoulides, G.I. Stegeman, A. Hach, R. Morandotti, H. Yang, G. Salamo, and M. Sorel, “Observation of Discrete Surface Solitons,” *Phys. Rev. Lett.* **96**, 063901 (2006).
5. Y. Lahini, E. Frumker, Y. Silberberg, S. Droulias, K. Hizanidis, R. Morandotti, and D.N. Christodoulides, “Discrete X-Wave Formation in Nonlinear Waveguide Arrays,”

- Phys. Rev. Lett. **98**, 023901 (2007).
6. S. Droulias, K. Hizanidis, J. Meier, and D.N. Christodoulides, “Xwaves in nonlinear normally dispersive waveguide arrays,” *Opt. Express* **13**, 1827-1832 (2005).
 7. J. Kutz, C. Conti, and S. Trillo, “Mode-locked X-wave lasers,” *Opt. Exp.* **15**, 16022-16028 (2007).
 8. S. Droulias, K. Hizanidis, D.N. Christodoulides, R. Morandotti, “Waveguide array-grating compressors,” *App. Phys. Lett.* **87**, 131104 (2005).
 9. J. Proctor and J. Kutz, “Passive mode-locking by use of waveguide arrays,” *Opt. Lett.* **30**, 2013 (2005).
 10. D. Marcuse, *Theory of dielectric optical waveguides*, 2nd Ed. (Boston, Academic Press, 1991).
 11. A. B. Aceves, C. De Angelis, T. Peschel, R. Muschall, F. Lederer, S. Trillo, and S. Wabnitz, “Discrete self-trapping, soliton interactions, and beam steering in nonlinear waveguide arrays,” *Phys. Rev. E* **53**, 1172-1189 (1996).
 12. H.S. Eisenberg, R. Morandotti, Y. Silberberg, J.M. Arnold, G. Pennelli, and J. S. Aitchison, “Optical discrete solitons in waveguide arrays. I. Soliton formation,” *J. Opt. Soc. Am. B* **19**, 2938-1944 (2002).
 13. U. Peschel, R. Morandotti, J.M. Arnold, J.S. Aitchison, H.S. Eisenberg, Y. Silberberg, T. Pertsch, and F. Lederer, “Optical discrete solitons in waveguide arrays. 2. Dynamics properties,” *J. Opt. Soc. Am. B* **19**, 2637-2644 (2002).
 14. F. Tauser, A. Leitenstorfer, and W. Zinth, “Amplified femtosecond pulses from an Er:fiber system: Nonlinear pulse shortening and selfreferencing detection of the carrier-

envelope phase evolution," Opt. Express **11**, 594-600 (2003).

Fig 1. (color online) Experimental setup. The output of the fiber laser is broadened by dispersion compensating fiber (DCF) to avoid nonlinearities in the amplifier. The grating compressor is tuned to produce a 600 fs pulse. The variable power control consists of a half-wave plate and a polarizer. A temporal intensity autocorrelation of the output pulses is recorded using a photomultiplier tube (PMT).

Fig 2. (color online) Measured power distribution at the output of the waveguide array. At low peak power the pulse in the center waveguide couples to neighboring waveguides. At high peak power, the pulse self-focuses in the central waveguide which results in a localized power distribution. The waveguide modes located symmetrically about the central waveguide had a symmetrical power distribution (not shown).

Fig 3. (color online) Autocorrelation signal versus waveguide number, with experimental results on the left ((a)-(c)) and theoretical simulations on the right ((d)-(f)). The three power levels shown correspond to those in Fig. 2, with (a) and (d) at 400 W, (b) and (e) at 720 W, and (c) and (f) at 1.5 kW. Pulse shortening in the center waveguide is observed in the 720 W and 1.5 kW cases. The autocorrelations are offset vertically for clarity, with the central waveguide being the lowest and the outer waveguides plotted sequentially higher on the vertical scale.

Fig 4. (color online) Output autocorrelation of central waveguide for input powers of 400 W, 720 W, 1 kW, and 1.5 kW. The inset shows the autocorrelation FWHM as a function of input power. The dotted trace is an autocorrelation of the input pulse.

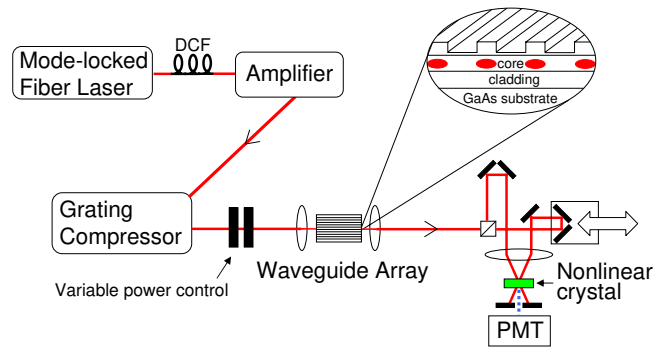


Fig. 1.

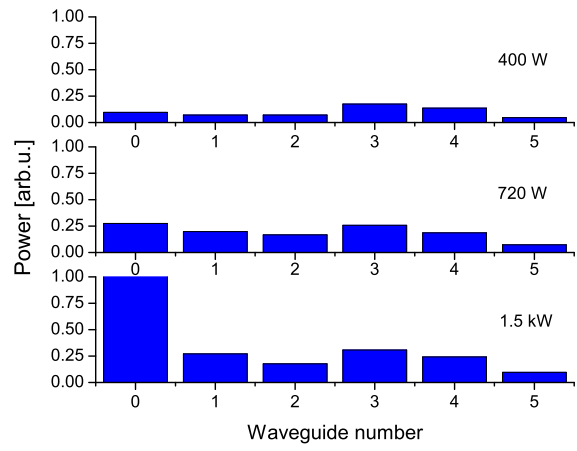


Fig. 2.

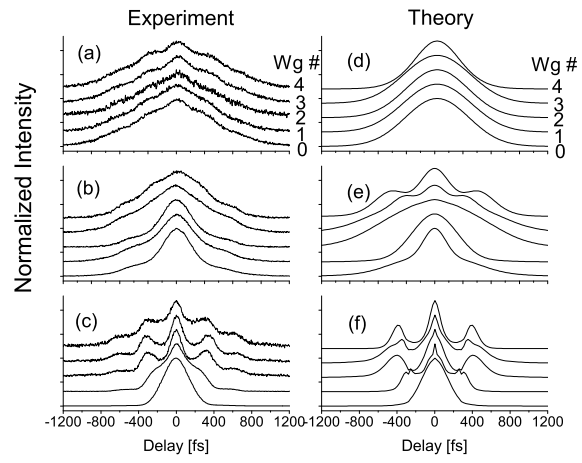


Fig. 3.

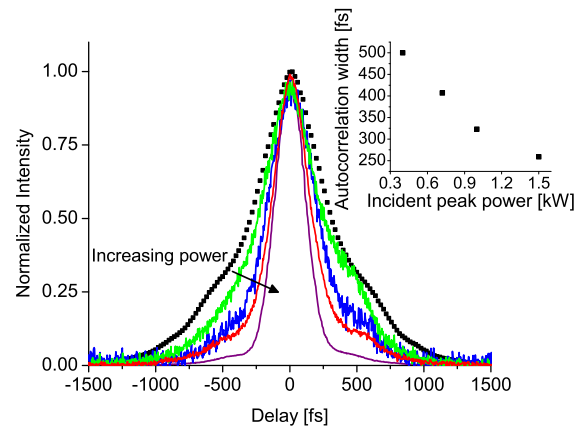


Fig. 4.